*Clays and Clay Minerals*, Vol. 65, No. 2, 92–103, 2017.

# MEASUREMENT OF SWELLING OF INDIVIDUAL SMECTITE TACTOIDS *IN SITU* USING ATOMIC FORCE MICROSCOPY

DIANA S. ARNDT, MICHAEL MATTEI, CHRISTOPHER A. HEIST, AND MOLLY M. MCGUIRE*
Department of Chemistry, Bucknell University, Lewisburg, PA 17837, USA

**Abstract**—Atomic force microscopy (AFM) is a novel method for measuring changes in clay swelling *in situ* at the tactoid level in an aqueous environment. While the swelling process has been directly observed at the mesoscale level for multi-tactoid aggregates and the associated pores, no method to date has allowed the direct observation of swelling dynamics at the nanoscale. In initial proof-of-concept studies, individual tactoids of a Na-exchanged nontronite (NAu-1) were imaged in a solution of 5 mM NaCl. When multiple line profiles were examined on the same tactoid, the changes in height varied and depended on which layers of the profile were transected, and demonstrated that AFM analyses can be used to directly probe intra-tactoid heterogeneity in the swelling process. To better visualize this heterogeneity, a method was developed to restrict AFM images to include only the portions of a tactoid above a threshold height. A comparison of the changes in these images for multiple threshold values revealed that swelling in one part of a tactoid may occur simultaneously with compression in another portion, which suggests that the encroachment of layers into intra-tactoid micropores can partially compensate for the overall volume change. Finally, to demonstrate the ability of this technique to monitor *in situ* swelling changes as the surrounding aqueous environment is modified, a tactoid of K-montmorillonite (SWy-2) was monitored during cation exchange as a KCl solution was replaced with NaCl. After exchange, a transition from the crystalline swelling regime to the osmotic regime was observed. Subsequent height profiles were unchanged for a period of several hours and indicated that the AFM measurements were stable in the absence of changes to the aqueous phase composition. Because this technique is the first method that allows the swelling of a single tactoid to be monitored in an aqueous solution, it complements the ensemble-averaged data obtained from diffraction and scattering techniques.

**Key Words**—Atomic Force Microscopy (AFM), Cation Exchange, Smectites, Swelling, Tactoid.

## INTRODUCTION

The phenomenon of clay swelling is of interest to scientists and engineers in a wide range of fields due to the role smectites play in soil health (Sparks, 2003), contaminant fate (*e.g.*, Chappell *et al.*, 2005; Chatterjee *et al.*, 2008), barrier technologies (Pusch, 2008; Bouazza and Bowders, 2010), and borehole stability (Durand *et al.*, 1995; Anderson *et al.*, 2010). In clay gels, the semi-oriented stacks of clay layers form tactoids and groups of these tactoids that are randomly oriented can form larger aggregates (Bihannic *et al.*, 2001a; Jullien *et al.*, 2005; Salles *et al.*, 2008; Salles *et al.*, 2010). Within individual tactoids, micropores with sizes on the order of several to tens of nanometers separate smaller stacks of more closely associated clay layers (Bihannic *et al.*, 2001b). The local ordering of clay gels with a liquid-like lamellar structure results from the mutual electrostatic repulsion of the clay platelets (Michot *et al.*, 2013b).

Clay swelling occurs in two regimes. Crystalline swelling, characterized by d-spacings on the order of ~17–20 Å, occurs when 1–4 layers of water accompany the cations in the interlayer region of the tactoid (MacEwan and Wilson, 1980). When smectites are in an aqueous environment, osmotic pressure between the aqueous environment and the interlayer region can force more water between layers and cause a greater degree of swelling known as osmotic swelling (Norrish and Rausell-Colom, 1963). Not all interlayer cations support osmotic swelling due to the balance of forces between the hydration of the cation and electrostatic attraction to the mineral surface (Boek *et al.*, 1995). Strongly hydrated cations, such as $Na^+$, support osmotic swelling, while $K^+$ tends to form inner-sphere complexes with the mineral surfaces and does not support osmotic swelling (MacEwan and Wilson, 1980). Osmotic swelling is characterized by d-spacings larger than ~40 Å and can result in the complete separation of clay layers (Norrish, 1954; Paumier *et al.*, 2008).

Because of the fundamental importance of swelling in soils and sediments, numerous studies of swelling have appeared in the literature in the past several decades. In laboratory investigations of smectites, gravimetric and calorimetric measurements in adsorption isotherms (*e.g.*, Cases *et al.*, 1992; Berend *et al.*, 1995; Komadel *et al.*, 2002; Michot *et al.*, 2005; Likos and Lu, 2006; Salles *et al.*, 2008; Salles *et al.*, 2009) and X-ray diffraction (*e.g.*, Norrish and Quirk, 1954; Posner and Quirk, 1964; Slade *et al.*, 1991; Zhang *et al.*, 1995; Bray *et al.*, 1998; Komadel *et al.*, 2002; Ferrage *et al.*, 2005; Amorim *et*

* E-mail address of corresponding author:
mmcguire@bucknell.edu
DOI: 10.1346/CCMN.2017.064053

*al.*, 2007; Ferrage *et al.*, 2007; Morodome and Kawamura, 2009; Morodome and Kawamura, 2011) have been frequently employed. While traditional X-ray diffraction techniques provide a means to monitor changes in interlayer spacing within tactoids through the crystalline stages of swelling, small angle X-ray scattering (SAXS) extends the length range of the scales probed to include the osmotic stage of swelling (*e.g.* Norrish, 1954; Hight *et al*., 1962; Rausell-Colom and Norrish, 1962; Norrish and Rausell-Colom, 1963; Andrews *et al.*, 1967; Pons *et al*., 1981; Pons *et al*., 1982; Morvan *et al*., 1994; Faisandier *et al*., 1998; Bihannic *et al.*, 2001b; Michot *et al.*, 2006; Segad *et al*., 2010; Paineau *et al.*, 2011; Segad *et al*., 2012). Similarly, small-angle neutron scattering (SANS) has provided additional information about the structure of clay aggregates at larger spatial scales than those that can be accessed by diffraction (Cebula *et al*., 1980; De Stefanis *et al*., 2007; Bihannic *et al*., 2008).

The ability of X-ray and neutron scattering techniques to probe mesoscopic structures have produced new insights into smectite-water systems. In particular, the heterogeneous structure of smectite gels or regions of closely associated layers in an extended network of pores that can span both within and between individual tactoids (Tessier, 1990; Morvan *et al*., 1994; Bihannic *et al*., 2001b) requires a swelling model that includes pore hydration at multiple size scales (Salles *et al*., 2008; Salles *et al*., 2010). As suggested by water sorption experiments, water uptake does not always lead to a macroscopic volume increase because interlamellar swelling occurs at the expense of the larger pores in the clay/water structure (Likos and Lu, 2006; Likos and Wayllace, 2010). Recently, Massat *et al.* (2016) used X-ray microtomography with a 5 μm spatial resolution to directly visualize decreases in inter-aggregate porosity during montmorillonite swelling.

At smaller length scales, the structural changes within individual tactoids during the swelling process have not yet been directly observed. Microscopy techniques that include scanning electron microscopy (SEM) (Baker *et al.*, 1995; Paumier *et al.*, 2008), laser scanning microscopy (LSM) (Suzuki *et al.*, 2005), X-ray fluorescence microscopy (Bihannic *et al*., 2001a), and transmission X-ray microscopy (TXM) using a synchrotron source (Zbik *et al.*, 2008, 2010; Michot *et al*., 2013a) have provided opportunities to visualize smectite tactoids and larger aggregates in suspensions and gels. Segad *et al.* (2012) demonstrated the use of cryo-transmission electron microscopy (cryo-TEM) to resolve the individual smectite layers in cryogenically prepared samples, but to date, no technique has been demonstrated for directly measuring nanometer-scale changes in the swelling of individual smectite tactoids *in situ* as the chemical composition of the aqueous phase is manipulated.

The work presented here demonstrates for the first time the use of atomic force microscopy (AFM) as a method for measuring the swelling of individual tactoids in aqueous solutions. AFM is a robust tool for studying environmentally relevant mineral-water interfaces (Maurice, 1996, 1998; Hochella *et al.*, 1998). This scanned probe technique uses the interatomic forces between a cantilever-mounted tip and the sample surface to map the topography of a surface (Sarid, 1994; Maurice, 1996). In previous studies of phyllosilicate minerals, AFM has been used to characterize particle size and morphology (*e.g.*, Lindgreen *et al.*, 1991, 2002; Cuadros and Altaner, 1998; Plaschke *et al.*, 2001; Balnois *et al.*, 2003; Piner *et al.*, 2003; Tournassat *et al.*, 2003; Krekeler *et al.*, 2004, 2005; Cadene *et al.*, 2005; Metz *et al.*, 2005; Hassan *et al.*, 2006; Ploehn and Liu, 2006; Can *et al.*, 2010; Gupta *et al.*, 2010; Marty *et al.*, 2011) and has been shown to quantitatively determine surface areas that agree well with conventional surface area measurements made using the Brunauer-Emmett-Teller isotherm (BET) method (Brunauer et al., 1938; Bickmore *et al.*, 2002). The AFM technique also has proven to be useful in characterizing the products of inorganic chemical reactions on clay mineral surfaces (Gan *et al.*, 1996; Charlet *et al.*, 2002).

A handful of investigators have used AFM *in situ* to image phyllosilicates in an aqueous environment (Bickmore *et al.*, 1999, 2001; Rufe and Hochella, 1999; Brandt *et al.*, 2003; Aldushin *et al.*, 2004a, 2004b, 2007; Yokoyama *et al.*, 2005; Kuwahara, 2008); however, no previously published studies used AFM to investigate smectite swelling properties *in situ*. Notably, the method presented here is the first technique that allows changes in interlayer spacing within a single tactoid to be followed through time and thus provide a direct and visual nanoscale observation of swelling dynamics. Such information at the tactoid-level can complement the holistic picture of clay swelling produced by diffraction and scattering techniques, which provide data on the average ensemble of all particles in a sample.

The studies presented here demonstrate the use of *in situ* AFM to monitor the changes within individual smectite tactoids in an aqueous solution. By employing post-acquisition image analysis to isolate specific layers within the tactoids, changes in swelling can be correlated with specific locations within the tactoid in order to probe the internal changes in structure. These experiments were designed to investigate the degree of layer-to-layer heterogeneity in osmotic swelling with the goal to determine whether intra-tactoid porosity provides a mechanism to compensate for volume change analogous to the mesoscale change which occurs between smectite aggregates (Likos and Lu, 2006; Likos and Wayllace, 2010; Massat *et al*., 2016). The novel AFM method presented here should prove applicable to investigations of nearly any process in a clay/water system. As an example, the ability to exchange solutions in the AFM

https://doi.org/10.1346/CCMN.2017.064053 Published online by Cambridge University Press

fluid cell without removing the particle from the aqueous environment was demonstrated using a cation exchange experiment.

## MATERIALS AND METHODS

Samples of the nontronite (NAu-1) and montmorillonite (SWy-2) were purchased from the Source Clays Repository of The Clay Minerals Society. Previous studies determined the smectite formulas as follows:

NAu-1 $M^{+}_{1.02}[Si_{6.98}Al_{0.95}Fe_{0.07}][Al_{0.36}Fe_{3.61}Mg_{0.04}]O_{20}(OH)_4$ (Gates *et al*., 2002)

SWy-2 $M^{+}_{0.70}[Si_{7.83}Al_{0.17}][Al_{3.02}Fe_{0.45}Mg_{0.53}]O_{20}(OH)_4$ (Geramian *et al.*, 2016).

The NAu-1 sample was purified by size fractionation using a wet sedimentation process (Vaniman, 2001). Both clays were treated with 0.1 M acetic acid to remove carbonate impurities and rinsed in 18 MΩ·cm water in triplicate. Cation exchange was achieved by washing with 1 M chloride solutions containing the desired interlayer cation followed by triplicate rinses. Samples were then dried in air at room temperature.

To prepare samples for AFM analysis, discrete tactoids were deposited on either a sapphire substrate or a modified mica disk (Bickmore *et al*, 1999). At circumneutral pH (6.5−7.5), the sapphire substrate has a positive surface charge which holds the negatively charged clay mineral in place by electrostatic attraction with the basal surface that is oriented parallel to the substrate. Mica disks treated with a poly(ethyleneimine) (PEI) solution exhibit a similar electrostatic attraction that adequately secures clay particles to the substrate. Grade V-4 15 mm diameter mica disks (SPI Supplies; West Chester, Pennsylvania, USA) were split before application of the PEI solution to provide a freshly cleaved surface. The mica disks were then soaked in a 1:2000 PEI solution diluted from a 50% (w/v) PEI solution in $H_2O$ (Sigma-Aldrich, St. Louis, Missouri, USA) for ~30 seconds. Each disk was then rinsed with a stream of 18 MΩ·cm water for 1 min and dried in an oven at 90ºC for 20 min. A 30 min ultrasonic treatment was used to prepare suspensions that contained 5 mg of purified clay in 150 mL of 18 MΩ·cm water for each of the NAu-1 and SWy-2 clays. Using a syringe, 2−5 drops of the desired clay suspension were loaded onto the sapphire or PEI-coated mica substrate and allowed to dry in a desiccator overnight. Solutions of 5 mM NaCl or KCl for use in the AFM fluid cell were prepared in 18 MΩ·cm water.

AFM images were acquired with a fluid cell using a Multimode V scanning probe microscope with a Nanoscope V controller (Bruker, Billerica, Massachusetts, USA) and equipped with Multi75-G Silicon AFM probes with resonant frequencies of ~75 kHz in air and ~30 kHz in $H_2O$ (Budget Sensors; Sofia, Bulgaria). All data were acquired in intermittent contact mode in order to minimize lateral forces between the tip and sample that might displace the clay layers (Bickmore *et al*., 1999). Images were analyzed using WSxM 5.0 Develop 5.3 and 8.0 freeware (Horcas *et al.*, 2007). Uncertainty in height measurements was ± 0.5 nm based on the calibration of the AFM with a step-height standard.

## RESULTS

A Na-nontronite sample prepared as described above was analyzed after 5 mM NaCl was introduced into the fluid cell (Figure 1a) and a tactoid was revealed in the AFM image that remained anchored to the substrate with basal surfaces parallel to the underlying surface. Because the AFM image is a visual representation of the measured sample topography, the data can also be plotted as numerical values of the height (position on the *z* axis) as a function of the position in the *x*–*y* plane of the image. The height profile (Figure 1b) or vertical cross section provided measured height values that were taken along the line shown in the AFM image (Figure 1a). Note that the aspect ratio of this particle

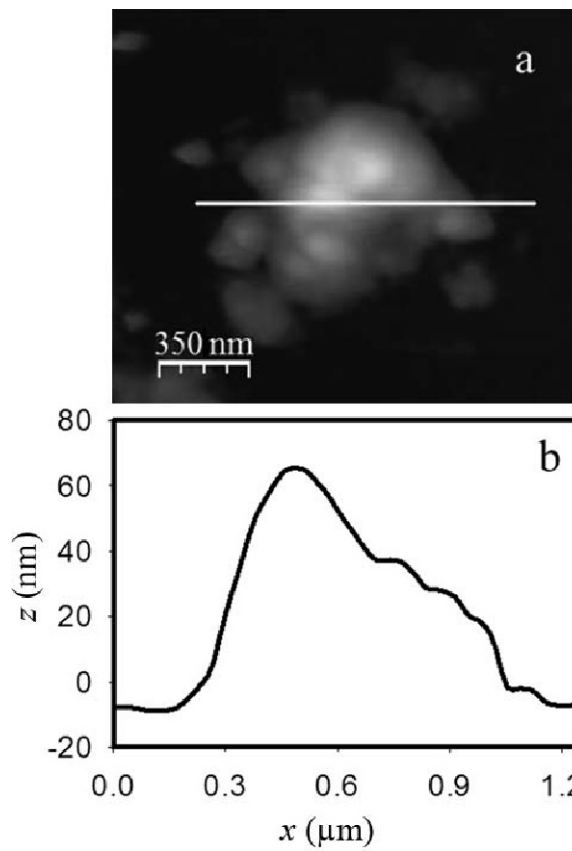


Figure 1. An AFM image (a) of a Na-exchanged NAu-1 tactoid in a solution of 5 mM NaCl. The height profile (b) corresponds to the line in the image (a).

https://doi.org/10.1346/CCMN.2017.064053 Published online by Cambridge University Press

was distorted in the height profile by the different scales in the axes used for the lateral (μm) and vertical (nm) dimensions. The stair-step pattern on the right-hand side of the height profile revealed the overlapped layers which comprised this tactoid. On the left-hand side of the height profile, however, no stair-step pattern was seen. In this case, the individual layers were hidden to the AFM. Presumably, this was because the stack was offset such that the layers above were overhanging layers that were farther down to produce an inverted staircase on this side of the tactoid.

The heights of the steps between the distinct terraces observed in the profile (Figure 1b) provided direct measurements of the separations between the exposed layers in the tactoid. Although these values varied widely from several nm to tens of nm, the layer spacings were all significantly larger than the ~40 Å spacing observed using XRD at the onset of osmotic swelling (Norrish, 1954). Because a clay layer with a smaller lateral area tucked underneath a larger exposed layer is possible and cannot be excluded, the steps measured in the height profile cannot be definitively assigned to the distances between nearest-neighbor layers.

Although comparisons between AFM height profiles allow for easy quantitative determinations of apparent changes in swelling along a line, the information provided is only a two-dimensional section of a three-dimensional tactoid. The height along the line measured using AFM represents the combined contributions from the uppermost layer that the line crossed and every layer beneath. Different layers may be exposed across the top surface of the tactoid due to the non-uniform particle morphology created by layers of different lateral dimensions which are not aligned with one another. If the swelling process is not uniform through all layers of the tactoid, a measured change in height profile may be a function of the location on the particle. This possibility was investigated for a NAu-1 tactoid (Figure 2a). The height profiles were measured at the spatial locations shown (Figure 2a) at two different times after the introduction of 5 mM NaCl to the fluid cell. On the left side of the particle (Figure 2b, 2c), the height profile at the later time was uniformly higher than the initial profile and indicated that particle height increased as the tactoid equilibrated with the solution. Conversely, the height profiles obtained further towards the right side of the particle (Figure 2d, 2e) indicated that the particle height decreased.

These data suggest that the swelling process is not uniform across the lateral dimensions of a smectite tactoid and, furthermore, that the choice of location of an AFM line profile affects the apparent degree of swelling that is measured. A closer examination of the AFM image (Figure 2), however, revealed that the four individual line profiles probed areas of the tactoid where different portions of the layer stacks were exposed. The AFM line profile furthest to the left side of the particle (Figure 2b, maximum height of 178 nm) transected layers farthest down in the tactoid structure, followed by the fourth line on the far right (Figure 2e, maximum height of 202 nm), the second line (Figure 2c, maximum height of 234 nm), and finally by the third line (Figure 2d, maximum height of 280 nm) which transected the topmost exposed layer. Consequently, the differences in the direction of change of the height profiles with time (Figure 2b–2e) can be correlated with the changes in the swelling state of a layer subset within the tactoid. In this particular case, there seems to have been significant variation in the swelling behavior which did not appear to be correlated to the vertical position within the tactoid.

The variability in the AFM height profiles obtained from different locations on the same tactoid suggests that additional information about the dynamics of the swelling process can be revealed through a more holistic approach to image analysis. An alternative approach to examining the two-dimensional slice of an image created from a line profile is to examine the change across the entire lateral dimension of the particle. By restricting the images to only points above a threshold value for the measured height, a comparison of the particle areas at two different times may reveal swelling if additional areas of the tactoid become apparent as the threshold height is achieved. Conversely, if a particle area exhibits layer compression, the area may disappear from the image as those points fall below the threshold height. By comparing different threshold values on the same particle, changes in the swelling state may be monitored as a function of vertical position within the tactoid layer stack.

This process of using multiple vertical thresholds for comparing images is illustrated for a Na-nontronite tactoid (Figure 3). Two images of the particle were acquired at approximately 10 min (Figure 3a) and 45 min (Figure 3b) after a solution of 5 mM NaCl was introduced into the fluid cell. To illustrate the height-dependent changes in the particle, the *flooding* function in the image analysis software was used to restrict points in the images to points at or above a certain plane, which made all points below the chosen plane a uniform background color (Figure 3c–3f). When the threshold plane was set at 40 nm (Figure 3c, 3d), a comparison of the images revealed that a larger fraction of the lateral area of the particle met this minimum value at the later time (Figure 3d). The lower exposed layers on the right side of the particle have moved up and changed the shape of the particle that was visible above the 40-nm threshold. This change was also confirmed by the surface area calculated using the software that increased from 652,900 (Figure 3c) to 664,000 $nm^2$ (Figure 3d). The change that was apparent in the higher layers in the stack was determined by setting the threshold plane to 60 nm (Figure 3e, 3f). In contrast to the observations at the lower level in the stack, a decrease in surface area from

https://doi.org/10.1346/CCMN.2017.064053 Published online by Cambridge University Press

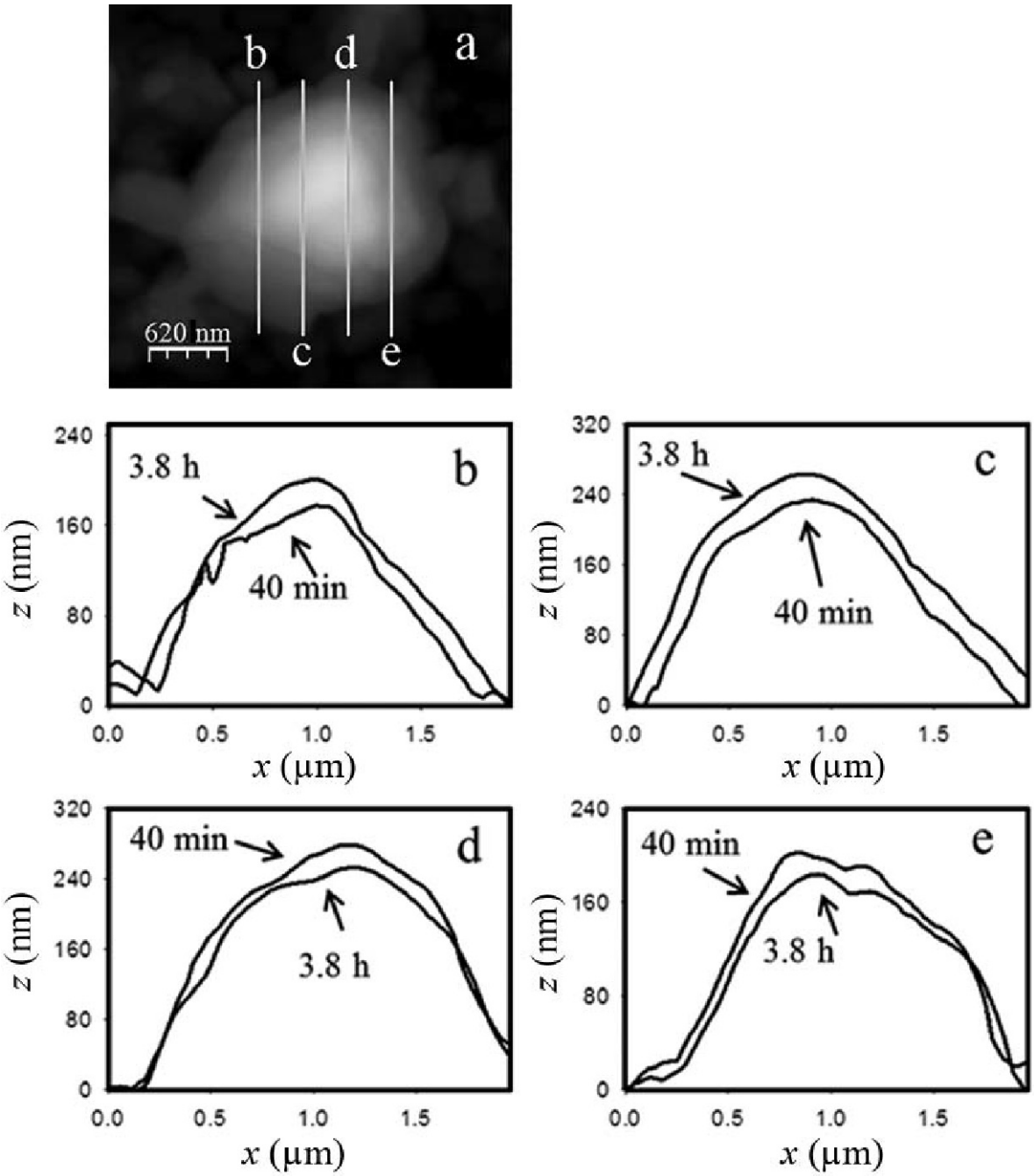


Figure 2. AFM image (a) and height profiles (b, c, d, e) across a Na-exchanged NAu-1 tactoid in 5 mM NaCl solution. The profiles indicate the particle heights 40 min and 3.8 h after the solution was introduced into the fluid cell.

401,200 (Figure 3e) to 350,200 nm$^2$ (Figure 3f) was apparent and suggested that some of the higher layers were compressed and dropped below the 60 nm threshold.

As another example, an identical experiment was performed on a second NAu-1 tactoid (Figure 4). Threshold values were chosen again based on the heights of the exposed lower layers in order to best illustrate the changes apparent in this particular tactoid. When the threshold value was set at 40 nm (Figure 4c, 4d), the particle surface area clearly increased during the 75 min exposure to a solution of 5 mM NaCl and the lateral surface area increased from 541,100 to 595,800 nm$^2$. A second plane at a threshold value of 60 nm (Figure 4e, 4f) indicated the same trend with a surface area increase from 300,800 to 378,800 nm$^2$. In contrast to the previous sample, all the exposed layers in this particle appeared to swell.

https://doi.org/10.1346/CCMN.2017.064053 Published online by Cambridge University Press

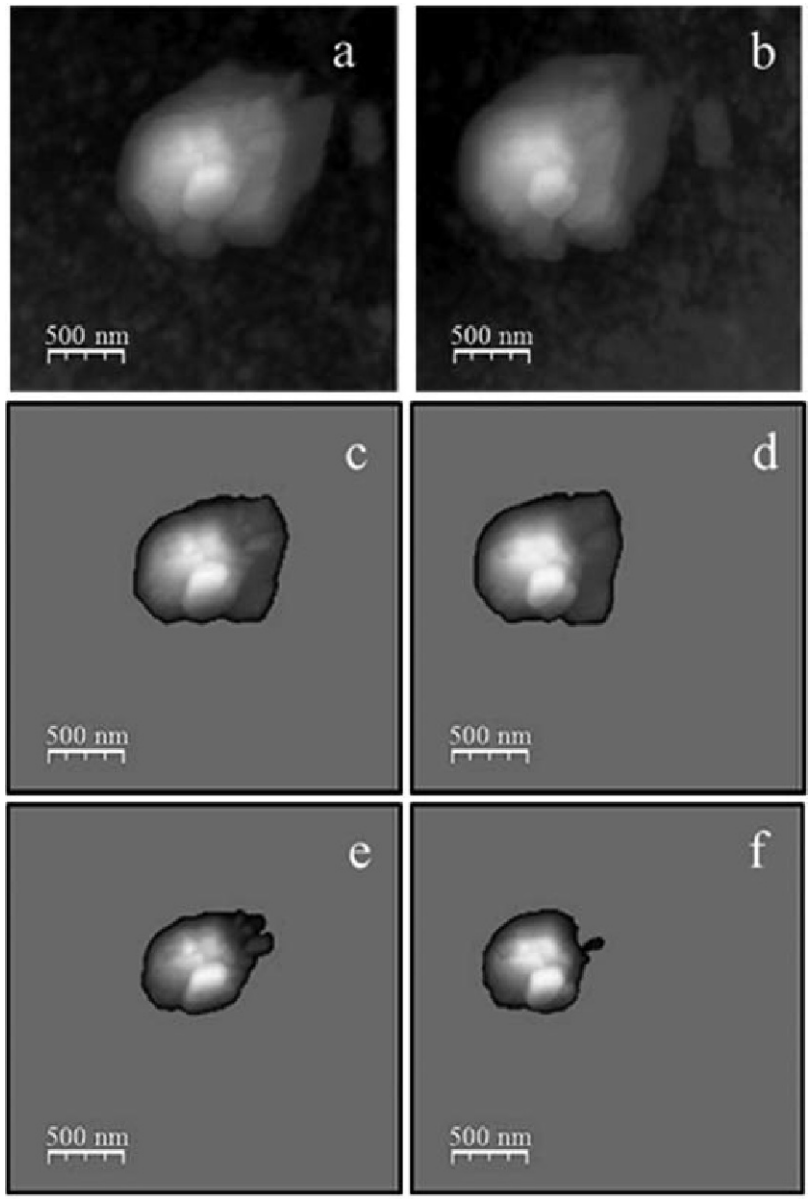


Figure 3. Flooded images of a Na-exchanged NAu-1 tactoid in a 5 mM NaCl solution produced by restricting the original AFM images only to points above a threshold height. The original images were acquired 10 min (a) and 45 min (b) after the solution was introduced into the fluid cell. The flooded images indicate the particle area 10 min (c) and 45 min (d) after the solution was introduced at the 40-nm plane and 10 min (e) and 45 min (f) after the solution was introduced at the 60-nm plane.

Taken together, the data presented here (Figures 1–4) demonstrated that AFM provides a method to directly measure swelling at multiple points within a single smectite tactoid. The primary advantage that this technique offers is the ability to make these measurements *in situ* as the aqueous environment is modified. The cation exchange process, which directly affects swelling, is an example of a dynamic process that could be explored using this technique. To illustrate this use of the technique, a K-montmorillonite tactoid was initially equilibrated in a 5 mM solution of KCl in the fluid cell and the particle was imaged (Figure 5 inset). The solution in the fluid cell was exchanged and the tactoid was imaged again after equilibration for 1.5 h in 5 mM NaCl. As can be clearly seen in the height profiles (Figure 5), the overall height of the tactoid increased by ~10 nm after equilibration with NaCl solution. Two subsequent AFM images of the tactoid in NaCl were taken along the same line and these profiles (Figure 5) were almost perfectly aligned with the profile measured at 1.5 h and indicated that the clay exhibited no further changes in swelling after an additional 3 or 4 h.

https://doi.org/10.1346/CCMN.2017.064053 Published online by Cambridge University Press

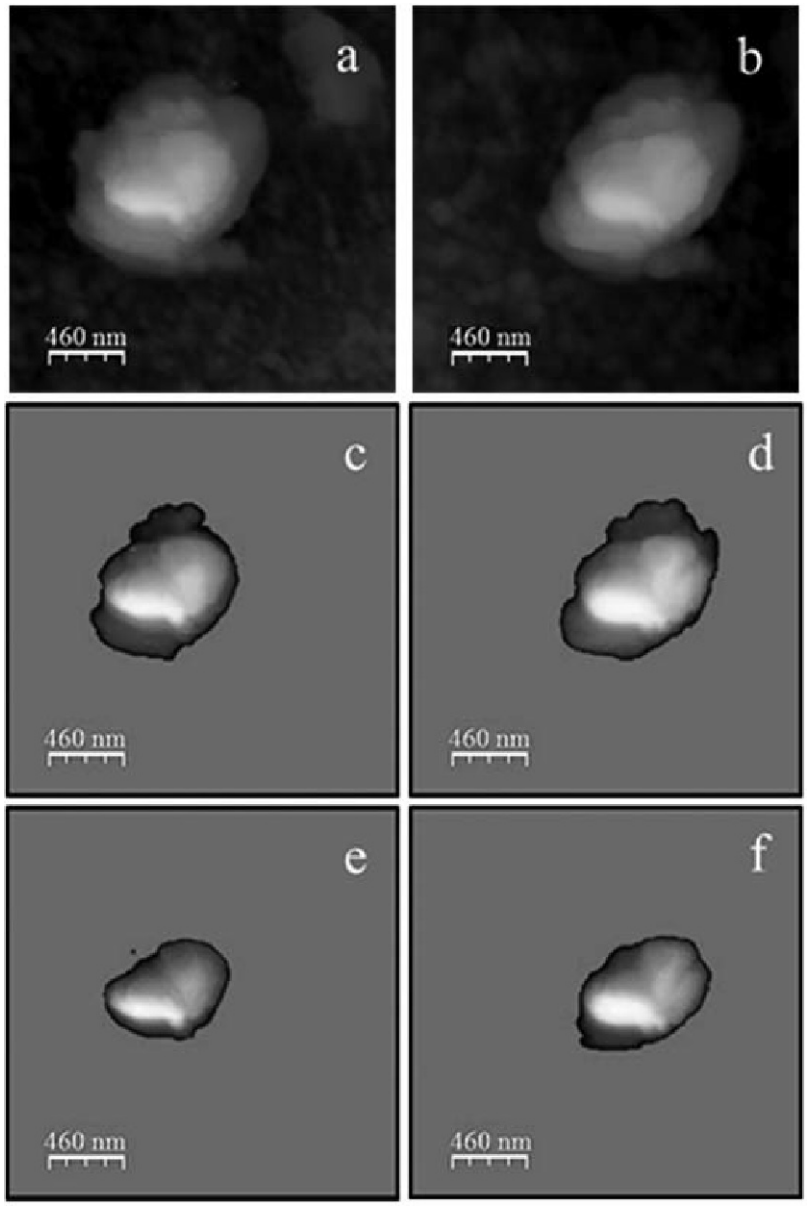


Figure 4. Flooded images of a Na-exchanged NAu-1 tactoid in a 5 mM NaCl solution produced by restricting the original AFM images to only points above a threshold height. The original images were acquired 25 min (a) and 75 min (b) after the solution was introduced into the fluid cell. The flooded images indicate the particle area 25 min (c) and 75 min (d) after the solution was introduced at the 40-nm plane and 25 min (e) and 75 min (f) after the solution was introduced at the 60-nm plane.

## DISCUSSION

### *Tactoid microstructure*

The AFM images of smectite samples obtained by the method described here revealed the presence of isolated particles anchored to the underlying substrate. The particles, which have significantly larger lateral dimensions than height, have a terraced structure that indicated the particles were composed of stacks of clay layers. The stability of the particles suggests that the particles were indeed tactoids, although the data do not definitively prove that these particles were truly individual tactoids formed from layers that were closely associated, mutually attracted, and not aggregates of layers that were randomly deposited together. Neither the introduction of an aqueous solution to the fluid cell nor the equilibration of the particle in that solution broke up these structures. Furthermore, the ionic strength of the solutions used here (5 mM NaCl) was chosen in order to support the formation of tactoids. Similar salt concentrations have been shown to lead to coagulation of the initially dispersed Na-montmorillonite layers in suspensions (Michot *et al*., 2013a).

https://doi.org/10.1346/CCMN.2017.064053 Published online by Cambridge University Press

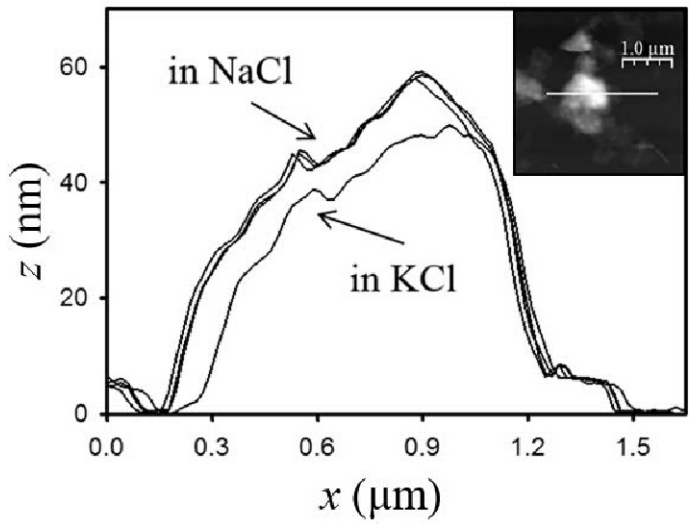


Figure 5. Height profiles of a K-exchanged SWy-2 tactoid first equilibrated in 5 mM KCl and then equilibrated for 1.5, 3, and 4 h after 5 mM NaCl was introduced into the fluid cell with the AFM image inset in the upper right corner.

The distance that separated the exposed terraces in these particles varied considerably and suggests that the internal structure of the tactoids were not uniform distributions of clay layers. The larger separations may be due to micropores that separate the domains of more closely associated layers. This interpretation was supported by SAXS studies of both dried montmorillonite films (Bihannic *et al*., 2001b) and particles in suspension (Faisandier *et al*., 1998; Michot *et al*., 2013a) which provided evidence of internal porosity within individual particles.

*Swelling heterogeneity*

The AFM technique demonstrated here provides a method of directly measuring the physical dimensions of a clay mineral tactoid in an aqueous environment. Although changes in the overall size of a particle (*i.e.* the measured height of the exposed surface at the top of the tactoid relative to the underlying substrate) can be readily determined from a comparison of AFM images, interpreting the changes in height as a change in layer separation requires a careful examination of the particle morphology. Because the tactoids deposited on the substrate by this sample preparation method are composed of layers with various lateral dimensions that are randomly aligned with respect to the x-y plane, the exposed upper surface of the particle often consists of the parts of multiple layers at different levels in the stack. In these cases, changes in measured height can then be related to changes in layer spacing for different portions of the particle. These position-dependent changes can be monitored either by examination of multiple line profiles that transect different layers (Figure 2) or by setting different threshold values for the height data and comparing the changes in particle lateral area at those specific planes (Figures 3, 4).

Regardless of which analysis method is employed, the data presented here indicates that the swelling process does not proceed uniformly throughout all layers of a tactoid. As a tactoid equilibrates with an aqueous solution, layer separation may increase in some layers while the distances between other layers may decrease. Swelling thus does not proceed as a uniform increase in the measured height of every exposed layer, but rather results in both increases and decreases of the vertical position of individual layers even as the tactoid as a whole increases in volume.

The variability in swelling response is likely due to the initial, heterogeneous microstructure of the tactoids, which as discussed above are likely composed of substacks of closely associated layers separated by lenticular micropores (Bihannic *et al*., 2001b). These micropores provide regions into which neighboring layers can expand and effectively compress one area of the tactoid even as the overall volume increases. This picture of swelling at the scale of individual tactoids is analogous to the swelling process observed at the micrometer scale where larger inter-particle pores decrease in size as interlayer swelling proceeds (Likos and Lu, 2006; Likos and Wayllace, 2010; Massat, 2016).

*Applications and limitations of the method*

As illustrated by changes in the measured height profiles in the cation exchange experiment (Figure 5), the AFM measurement technique provides sufficient stability to monitor changes over extended time periods without interferences due to non-chemical changes. The only change observed in this experiment took place sometime within the first 1.5 h of equilibration in NaCl as $Na^+$ from the aqueous environment around the clay diffused into the interlayer and exchanged for the original $K^+$ cations. Presumably, the solution exchange

https://doi.org/10.1346/CCMN.2017.064053 Published online by Cambridge University Press

in the fluid cell provided a significant excess of aqueous phase $Na^+$ in comparison to $K^+$ and a large fraction of the $K^+$ was leached from the clay upon equilibration. Once a sufficient amount of Na entered the interlayer, the tactoid transitioned from the crystalline to the osmotic swelling regime that is supported by $Na^+$ but not by $K^+$ (MacEwan and Wilson, 1980; Boek *et al.*, 1995). Once this equilibration was complete, no additional change in the swelling state was observed, which demonstrated the sensitivity and specificity of the technique to measure swelling changes that result from modification of the aqueous phase composition.

The stability of the AFM measurements in combination with the *in situ* fluid cell flexibility allows solution exchange at any desired interval and makes this method uniquely useful for studying changes in swelling that accompany a change in the aqueous phase composition. With more frequent imaging (at minute rather than hour intervals), this technique could be used to obtain kinetics data for the exchange of interlayer cations and the transitions from one swelling regime to another. Additionally, because AFM allows a single tactoid to be followed through time, the technique presented here can complement XRD and SAXS studies, which provide average information on the ensemble of all the clay layers in a sample. The direct visualization of structural changes at the scale of individual tactoids using AFM can provide confirmation of models used to interpret diffraction and scattering data.

The most significant limitation of AFM use to monitor clay mineral swelling is the dependence on tactoid morphology, which cannot be controlled in the sample preparation process. The ability of the technique to measure the heights of multiple layers within a single tactoid requires that a tactoid be found in which the layer stack is aligned with multiple layers that are exposed on the top surface of the particle. Tactoids deposited onto the substrate from a suspension as the sample evaporates form completely random stacks. When smaller layers end up underneath broader layers, the layers are not accessible to the AFM tip and as a consequence the individual changes in swelling cannot be determined. A judicious choice of tactoids for imaging is necessary in order to maximize the information that can be obtained from AFM analyses.

## CONCLUSIONS

AFM is a novel *in situ* method for directly measuring clay mineral swelling at the tactoid level in an aqueous environment. Analysis of multiple layers within a single tactoid revealed that osmotic swelling at the nanoscale is a heterogeneous process and significant variability was observed at different locations within the tactoid. An increase in the layer spacing in one region may result in a decrease in the spacing in a neighboring region, which suggests that the internal porosity within a tactoid may be lost during swelling. The method, which is unique in its ability to monitor a single tactoid in an aqueous solution, is applicable to studies of any system in which a changing aqueous environment will modify the degree of swelling. AFM analyses complement the ensemble-averaged information obtained from diffraction and scattering studies and offer opportunities for *in situ* studies of the role of smectites in contaminant fate and transport as well as kinetics studies of individual tactoids.

## ACKNOWLEDGMENTS

Financial support for this work was provided by the National Science Foundation (EAR-1053140).

## REFERENCES

Aldushin, K., Jordan, G., Aldushina, E., and Schmahli, W.W. (2007) On the kinetics of ion exchange in phlogopite – An *in situ* AFM study. *Clays and Clay Minerals*, **55**, 339–347.

Aldushin, K., Jordan, G., Fechtelkord, M., Schmahl, W.W., Becker, H.W., and Rammensee, W. (2004a) On the mechanisms of apophyllite alteration in aqueous solutions. A combined AFM, XPS and MAS NMR study. *Clays and Clay Minerals*, **52**, 432–442.

Aldushin, K., Jordan, G., Rammensee, W., Schmahl, W.W., and Becker, H.W. (2004b) Apophyllite (001) surface alteration in aqueous solutions studied by HAFM. *Geochimica et Cosmochimica Acta*, **68**, 217–226.

Amorim, C.L.G., Lopes, R.T., Barroso, R.C., Queiroz, J.C., Alves, D.B., Perez, C.A., and Schelin, H.R. (2007) Effect of clay-water interactions on clay swelling by X-ray diffraction. *Nuclear Instruments & Methods in Physics Research Section A-Accelerators Spectrometers Detectors and Associated Equipment*, **580**, 768–770.

Anderson, R.L., Ratcliffe, I., Greenwell, H.C., Williams, P.A., Cliffe, S., and Coveney, P.V. (2010) Clay swelling - A challenge in the oilfield. *Earth-Science Reviews*, **98**, 201–216.

Andrews, D.E., Schmidt, P.W., and Van Olphen, H. (1967) X-ray study of interactions between montmorillonite platelets. *Clays and Clay Minerals* **15**, 321–330.

Baker, J.C., Grabowskaolszewska, B., and Uwins, P.J.R. (1995) ESEM Study of osmotic swelling of bentonite from Radzionkow (Poland). *Applied Clay Science*, **9**, 465–469.

Balnois, E., Durand-Vidal, S., and Levitz, P. (2003) Probing the morphology of laponite clay colloids by atomic force microscopy. *Langmuir*, **19**, 6633–6637.

Berend, I., Cases, J.M., Francois, M., Uriot, L.M., Masion, A., and Thomas, F. (1995) Mechanism of adsorption and desorption of water vapor by homoionic montmorillonites. 2. The $Li^+$, $Na^+$, $K^+$, $Rb^+$ and $Cs^+$-exchanged forms. *Clays and Clay Minerals*, **43**, 324–336.

Bickmore, B.R., Hochella, M.F., Bosbach, D., and Charlet, L. (1999) Methods for performing atomic force microscopy imaging of clay minerals in aqueous solution. *Clays and Clay Minerals*, **47**, 573–581.

Bickmore, B.R., Bosbach, D., Hochella, M.F., Jr, Charlet, L., and Rufe, E. (2001) *In situ* atomic force microscopy study of hectorite and nontronite dissolution: Implications for phyllosilicate edge surface structures and dissolution mechanisms. *American Mineralogist*, **86**, 411–423.

Bickmore, B.R., Nagy, K.L., Sandlin, P.E., and Crater, T.S. (2002) Quantifying surface areas of clays by atomic force microscopy. *American Mineralogist*, **87**, 780–783.

Bihannic, I., Michot, L.J., Lartiges, B.S., Vantelon, D., Labille,

J., Thomas, F., Susini, J., Salome, M., and Fayard, B. (2001a) First direct visualization of oriented mesostructures in clay gels by synchrotron-based X-ray fluorescence microscopy. *Langmuir*, **17**, 4144–4147.

Bihannic, I., Tchoubar, D., Lyonnard, S., Besson, G., and Thomas, F. (2001b) X-ray scattering investigation of swelling clay fabric 1. The dry state. *Journal of Colloid and Interface Science*, **240**, 211–218.

Bihannic, I., Delville, A., Demé, B., Plazanet, M., Villiéras, F., and Michot, L.J. (2008) Clay swelling: New insights from neutron-based techniques. Pp. 521–546 in: *Neutron Applications in Earth, Energy and Environmental Sciences* (L. Liyuan, R. Rinaldi, and H. Schober, editors). Springer, New York.

Boek, E.S., Coveney, P.V., and Skipper, N.T. (1995) Monte Carlo molecular modeling studies of hydrated Li-, Na-, and K-smectites: Understanding the role of potassium as a clay swelling inhibitor. *Journal of the American Chemical Society*, **117**, 12608–12617.

Bouazza A. and Bowders J.J., Jr. (2010) *Geosynthetic Clay Liners for Waste Containment Facilities*. CRC Press, Boca Raton, Florida, USA, 254 pp.

Brandt, F., Bosbach, D., Krawczyk-Barsch, E., Arnold, T., and Bernhard, G. (2003) Chlorite dissolution in the acid pH-range: A combined microscopic and macroscopic approach. *Geochimica et Cosmochimica Acta*, **67**, 1451–1461.

Bray, H.J., Redfern, S.A.T., and Clark, S.M. (1998) The kinetics of dehydration in Ca-montmorillonite: an *in situ* X-ray diffraction study. *Mineralogical Magazine*, **62**, 647–656.

Brunauer, S., Emmett, P.H., and Teller, E. (1938) Adsorption of gases in multimolecular layers. *Journal of the American Chemical Society*, **60**, 309–319.

Cadene, A., Durand-Vidal, S., Turq, P., and Brendle, J. (2005) Study of individual Na-montmorillonite particles size, morphology, and apparent charge. *Journal of Colloid and Interface Science*, **285**, 719–730.

Can, M.F., Cinar, M., Benli, B., Ozdemir, O., and Celik, M.S. (2010) Determining the fiber size of nano structured sepiolite using atomic force microscopy (AFM). *Applied Clay Science*, **47**, 217–222.

Cases, C.M., Berend, I., Besson, G., Francois, M., Uriot, J.P., Thomas, F., and Poirier, J.E. (1992) Mechanism of adsorption and desorption of water vapor by homoionic montmorillonite. 1. The sodium-exchanged form. *Langmuir*, **8**, 2730–2739.

Cebula, D.J. and Thomas, R.K. (1980) Small angle neutron scattering from dilute aqueous dispersions of clay. *Journal of the Chemical Society, Faraday Transactions I*, **76**, 314–321.

Chappell, M.A., Laird, D.A., Thompson, M.L., Li, H., Teppen, B.J., Aggarwal, V., Johnston, C.T., and Boyd, S.A. (2005) Influence of smectite hydration and swelling on atrazine sorption behavior. *Environmental Science & Technology*, **39**, 3150–3156.

Charlet, L., Bosbach, D., and Peretyashko, T. (2002) Natural attenuation of TCE, As, Hg linked to the heterogeneous oxidation of Fe(II): an AFM study. *Chemical Geology*, **190**, 303–319.

Chatterjee, R., Laird, D.A., and Thompson, M.L. (2008) Interactions among $K^{+}$-$Ca^{2+}$ exchange, sorption of m-dinitrobenzene, and smectite quasicrystal dynamics. *Environmental Science & Technology*, **42**, 9099–9103.

Cuadros, J. and Altaner, S.P. (1998) Characterization of mixed-layer illite-smectite from bentonites using microscopic, chemical, and X-ray methods: Constraints on the smectite-to-illite transformation mechanism. *American Mineralogist*, **83**, 762–774.

De Stefanis, A., Tomlinson, A.A.G., Steriotis, Th.A., Charalambopoulou, G.Ch., and Keiderling, U. (2007) Study of structural irregularities of smectite clay systems by small-angle neutron scattering and adsorption. *Applied Surface Science*, **253**, 5633–5639.

Durand, C., Forsans, T., Ruffet, C., Onaisi, A., and Audibert, A. (1995) Influence of clays on borehole stability – a literature survey. 1. Occurrence of drilling problems physicochemical description of clays and of their interaction with fluids. *Revue De L Institut Francais Du Petrole*, **50**, 187–218.

Faisandier, K., Pons, C.H., Tchoubar, D., and Thomas, F. (1998) Structural organization of Na- and K-montmorillonite suspensions in response to osmotic and thermal stresses. *Clays and Clay Minerals*, **46**, 636–648.

Ferrage, E., Lanson, B., Sakharov, B.A., and Drits, V.A. (2005) Investigation of smectite hydration properties by modeling experimental X-ray diffraction patterns: Part I. Montmorillonite hydration properties. *American Mineralogist*, **90**, 1358–1374.

Ferrage, E., Lanson, B., Sakharov, B.A., Geoffroy, N., Jacquot, E., and Drits, V.A. (2007) Investigation of dioctahedral smectite hydration properties by modeling of X-ray diffraction profiles: Influence of layer charge and charge location. *American Mineralogist*, **92**, 1731–1743.

Gan, H., Bailey, G.W., and Yu, Y.S. (1996) Morphology of lead(II) and chromium(III) reaction products on phyllosilicate surfaces as determined by atomic force microscopy. *Clays and Clay Minerals*, **44**, 734–743.

Gates, W.P., Slade, P.G., Manceau, A., and Lanson, B. (2002) Site occupancies by iron in nontronites. *Clays and Clay Minerals*, **50**, 223–239.

Geramian, M., Osacky, M., Ivey, D.G., Liu, Q., and Etsell, T.H. (2016) Effect of swelling clay minerals (montmorillonite and illite-smectite) on non-aqueous bitumen extraction from Alberta oil sands. *Energy & Fuels*, **30**, 8083–8090.

Gupta, V., Hampton, M.A., Nguyen, A.V., and Miller, J.D. (2010) Crystal lattice imaging of the silica and alumina faces of kaolinite using atomic force microscopy. *Journal of Colloid and Interface Science*, **352**, 75–80.

Hassan, M.S., Villieras, F., Gaboriaud, F., and Razafitianamaharavo, A. (2006) AFM and low-pressure argon adsorption analysis of geometrical properties of phyllosilicates. *Journal of Colloid and Interface Science*, **296**, 614–623.

Hight, R., Jr., Higdon, W.T., Darley, H.C.H., and Schmidt, P.W. (1962) Small angle X-ray scattering from montmorillonite clay suspensions. *Journal of Chemical Physics*, **37**, 502–510.

Hochella, M.F., Rakovan, J.F., Rosso, K.M., Bickmore, B.R., and Rufe, E. (1998) New directions in mineral surface geochemical research using scanning probe microscopes. Pp. 37–56 in: *Mineral-Water Interfacial Reactions* (D.L. Sparks and T.J. Grundl, editors). American Chemical Society, Washington, D.C.

Horcas, I., Fernandez, R., Gomez-Rodriquez, J.M., Colchero, J., Gomez-Herrero, J., and Baro, A.M. (2007) WSXM: A software for scanning probe microscopy and a tool for nanotechnology. *Review of Scientific Instruments*, **78**, 013705–1-013705–8.

Jullien, M., Raynall, J., Kohler, E., and Bildstein, O. (2005) Physiochemical reactivity in clay-rich materials: Tools for safety assessment. *Oil & Gas Science and Technology*, **60**, 107–120.

Komadel, P., Hrobarikova, J., Smrcok, L., and Koppelhuber-Bitschnau, B. (2002) Hydration of reduced-charge montmorillonite. *Clay Minerals*, **37**, 543–550.

Krekeler, M.P.S., Guggenheim, S., and Rakovan, J. (2004) A microtexture study of palygorskite-rich sediments from the Hawthorne Formation, southern Georgia, by transmission

electron microscopy and atomic force microscopy. *Clays and Clay Minerals*, **52**, 263–274.

Krekeler, M.P.S., Hammerly, E., Rakovan, J., and Guggenheim, S. (2005) Microscopy studies of the palygorskite-to-smectite transformation. *Clays and Clay Minerals*, **53**, 92–99.

Kuwahara, Y. (2008) *In situ* observations of muscovite dissolution under alkaline conditions at 25–50 degrees C by AFM with an air/fluid heater system. *American Mineralogist*, **93**, 1028–1033.

Likos, W.J. and Lu, N. (2006) Pore-scale analysis of bulk volume change from crystalline interlayer swelling in $Na^{+}$- and $Ca^{2+}$-smectite. *Clays and Clay Minerals*, **54**, 515–528.

Likos, W.J. and Wayllace, A. (2010) Porosity evolution of free and confined bentonites during interlayer hydration. *Clays and Clay Minerals*, **58**, 399–414.

Lindgreen, H., Garnaes, J., Hansen, P.L., Besenbacher, F., Laegsgaard, E., Stensgaard, I., Gould, S.A.C., and Hansma, P.K. (1991) Ultrafine particles of North Sea illite-smectite clay investigated by STM and AFM. *American Mineralogist*, **76**, 1218–1222.

Lindgreen, H., Drits, V.A., Sakharov, B.A., Jakobsen, H.J., Salyn, A.L., Dainyak, L.G., and Kroyer, H. (2002) The structure and diagenetic transformation of illite-smectite and chlorite-smectite from North Sea Cretaceous-Tertiary chalk. *Clay Minerals*, **37**, 429–450.

MacEwan, D.M.C. and Wilson, M.J. (1980) Interlayer and intercalation complexes of clay minerals. Pp. 197–248 in: *Crystal Structures of Clay Minerals and their X-ray Identification*, (G.W. Brindley and G. Brown, editors). Mineralogical Society, London.

Marty, N.C.M., Cama, J., Sato, T., Chino, D., Villieras, F., Razafitianamaharavo, A., Brendle, J., Giffaut, E., Soler, J.M., Gaucher, E.C., and Tournassat, C. (2011) Dissolution kinetics of synthetic Na-smectite. An integrated experimental approach. *Geochimica et Cosmochimica Acta*, **75**, 5849–5864.

Massat, L., Cuisinier, O., Bihannic, I., Claret, F., Pelletier, M., Masrouri, F., and Gaboreau, S. (2016) Swelling pressure development and inter-aggregate porosity evolution upon hydration of a compacted swelling clay. *Applied Clay Science*, **124–125**, 197–210.

Maurice, P.A. (1996) Applications of atomic force microscopy in environmental colloid and surface chemistry. *Colloids and Surfaces A*, **107**, 57–75.

Maurice, P.A. (1998) Atomic force microscopy as a tool for studying the reactivities of environmental particles. Pp. 57–66 in: *Mineral–Water Interfacial Reactions* (D.L. Sparks and T.J. Grundl, editors). American Chemical Society, Washington, D.C.

Metz, V., Raanan, H., Pieper, H., Bosbach, D., and Ganor, J. (2005) Towards the establishment of a reliable proxy for the reactive surface area of smectite. *Geochimica et Cosmochimica Acta*, **69**, 2581–2591.

Michot, L.J., Bihannic, I., Pelletier, M., Rinnert, E., and Robert, J.L. (2005) Hydration and swelling of synthetic Na-saponites: Influence of layer charge. *American Mineralogist*, **90**, 166–172.

Michot, L.J., Bihannic, I., Maddi, S., Funari, S.S., Baravian, C., and Levitz, P. (2006) Liquid-crystalline aqueous clay suspensions. *Proceedings of the National Academy of Sciences*, **103**, 16101–16104.

Michot, L.J., Bihannic, I., Thomas, F., Lartiges, B.S., Waldvogel, Y., Caillet, C., Thieme, J., Funari, S.S., and Levitz, P. (2013a) Coagulation of Na-montmorillonite by inorganic cations at neutral pH. A combined transmission X-ray microscopy, small angle and wide angle X-ray scattering study. *Langmuir*, **29**, 3500–3510.

Michot, L.J., Paineau, E., Bihannic, I., Maddi, S., Duval, J.F.L., Baravian, C., Davidson, P., and Levitz, P. (2013b) Isotropic/nematic and sol/gel transitions in aqueous suspensions of size selected NAu1. *Clay Minerals*, **48**, 663–685.

Morodome, S. and Kawamura, K. (2009) Swelling behavior of Na- and Ca-montmorillonite up to 150 degrees by *in situ* X-ray diffraction experiments. *Clays and Clay Minerals*, **57**, 150–160.

Morodome, S. and Kawamura, K. (2011) *In situ* X-ray diffraction study of the swelling of montmorillonite as affected by exchangeable cations and temperature. *Clays and Clay Minerals*, **59**, 165–175.

Morvan, M., Espinat, D., Lambard, J., and Zemb, Th. (1994) Ultrasmall- and small-angle X-ray scattering of smectite clay suspensions. *Colloids and Surfaces A*, **82**, 193–203.

Norrish, K. (1954) The swelling of montmorillonite. *Discussions of the Faraday Society*, **18**, 120–133.

Norrish, K. and Quirk, J.P. (1954) Crystalline swelling of montmorillonite – use of electrolytes to control swelling. *Nature*, **173**, 255–256.

Norrish, K. and Rausell-Colom, J.A. (1963) Low-angle X-ray diffraction studies of the swelling of montmorillonite and vermiculite. *Proceedings of the 10th National Conference on Clays and Clay Minerals*, 123–149.

Paumier, S., Pantet, A., and Monnet, P. (2008) Evaluation of the organization of the homoionic smectite layers ($Na^{+}$ or $Ca^{2+}$) in diluted dispersions using granulometry, microscopy and rheometry. *Advances in Colloid and Interface Science*, **141**, 66–75.

Paineau, E., Bihannic, I., Baravian, C., Philippe, A.M., Davidson, P., Levitz, Funari, S.S., Rochas, C., and Michot, L.J. (2011) Aqueous suspensions of natural swelling clay minerals. 1. Structure and electrostatic interactions. *Langmuir*, **27**, 5562–5573.

Piner, R.D., Xu, T.T., Fisher, F.T., Qiao, Y., and Ruoff, R.S. (2003) Atomic force microscopy study of clay nanoplatelets and their impurities. *Langmuir*, **19**, 7995–8001.

Plaschke, M., Schafer, T., Bundschuh, T., Manh, T.N., Knopp, R., Geckeis, H., and Kim, J.I. (2001) Size characterization of bentonite colloids by different methods. *Analytical Chemistry*, **73**, 4338–4347.

Ploehn, H.J. and Liu, C. (2006) Quantitative analysis of montmorillonite platelet size by atomic force microscopy. *Industrial & Engineering Chemistry Research*, **45**, 7025–7034.

Pons, C.H., Rousseaux, F., and Tchoubar. D. (1981) Use of synchrotron radiation small-angle diffusion for the study of swelling of smectites 1. Study of the water–Na-montmorillonite system as a function of temperature. *Clay Minerals*, **16**, 23–42.

Pons, C.H., Rousseaux, F., and Tchoubar. D. (1982) Use of synchrotron radiation small-angle diffusion for the study of swelling of smectites. 2. Study of different water–smectite systems as a function of temperature. *Clay Minerals*, **17**, 327–338.

Posner, A. and Quirk, J. (1964) Changes in basal spacing of montmorillonite in electrolyte solutions. *Journal of Colloid Science*, **19**, 798–812.

Pusch R. (2008) *Geological Storage of Highly Radioactive Waste: Current Concepts and Plans.* Springer, Berlin, 379 pp.

Rausell-Colom, J.A. and Norrish, K. (1962) Low-angle diffractometer for studying the swelling of clay minerals. *Journal of Scientific Instruments*, **39**, 156–159.

Rufe, E. and Hochella, M.F. (1999) Quantitative assessment of reactive surface area of phlogopite during acid dissolution. *Science*, **285**, 874–876.

Salles, F., Beurroies, I., Bildstein, O., Jullien, M., Raynal, J., Denoyel, R., and Van Damme, H. (2008) A calorimetric study of mesoscopic swelling and hydration sequence in

solid Na-montmorillonite. *Applied Clay Science*, **39**, 186–201.

Salles, F., Douillard, J.M., Denoyel, R., Bildstein, O., Jullien, M., Beurroies, I., and Van Damme, H. (2009) Hydration sequence of swelling clays: Evolution of specific surface area and hydration energy. *Journal of Colloid and Interface Science*, **333**, 510–522.

Salles, F., Bildstein, O., Douillard, J.M., Jullien. M., Raynal, J., and Van Damme, H. (2010) On the cation dependence of interlamellar and interparticular water and swelling in smectite clays. *Langmuir*, **26**, 5028–5037.

Sarid D. (1994) *Scanning Force Microscopy: with Applications to Electric, Magnetic, and Atomic Forces*. Oxford, New York, 288 pp.

Segad, M., Jönsson, Bo, Åkesson, T., and Cabane, B. (2010) Ca/Na montmorillonite: structure, forces, and swelling properties. *Langmuir*, **26**, 5782–5790.

Segad, M., Hanski, S., Olsson, U., Ruokolainen, J., Akesson, T., and Jonsson, B. (2012) Microstructural and swelling properties of Ca and Na montmorillonite: (*in situ*) observations with cryo-TEM and SAXS. *Journal of Physical Chemistry C*, **116**, 7596–7601.

Slade, P.G., Quirk, J.P., and Norrish, K. (1991) Crystalline swelling of smectite samples in concentrated NaCl solutions in relation to layer charge. *Clays and Clay Minerals*, **39**, 234–238.

Sparks, D.L. (2003) *Environmental Soil Chemistry, 2nd edition*. Elsevier, San Diego, California, USA, 352 pp.

Suzuki, S., Prayongphan, S., Ichikawa, Y., and Chae, B.G. (2005) *In situ* observations of the swelling of bentonite aggregates in NaCl solution. *Applied Clay Science*, **29**, 89–98.

Tessier, D. (1990) Behaviour and microstructure of clay minerals. Pp. 387–415 in: *Soil Colloids and Their Associations in Aggregates* (M.F. DeBoodt, M.H.B. Hayes, and A. Herbillon, editors). Plenum, New York.

Tournassat, C., Neaman, A., Villieras, F., Bosbach, D., and Charlet, L. (2003) Nanomorphology of montmorillonite particles: Estimation of the clay edge sorption site density by low-pressure gas adsorption and AFM observations. *American Mineralogist*, **88**, 1989–1995.

Vaniman, D. (2001) *Environmental Restoration Project Standard Operating Procedure for Clay Mineral and Zeolite Separation*. SOP-09.05, ER2001-0148, Los Alamos National Laboratory, Los Alamos, New Mexico, USA.

Yokoyama, S., Kuroda, M., and Sato, T. (2005) Atomic force microscopy study of montmorillonite dissolution under highly alkaline conditions. *Clays and Clay Minerals*, **53**, 147–154.

Zbik, M.S., Martens, W.N., Frost, R.L., Song, Y., Chen, Y., and Chen, J. (2008) Transmission X-ray microscopy (TXM) reveals the nanostructure of a smectite gel. *Langmuir*, **24**, 8954–8958.

Zbik, M.S., Martens, W.N., Frost, R.L., Song, Y., Chen, Y., and Chen, J. (2010) Smectite flocculation structure modified by $Al_{13}$ macro-molecules – As revealed by the transmission X-ray microscopy (TXM). *Journal of Colloid and Interface Science*, **345**, 34–40.

Zhang, F.S., Low, P.F., and Roth, C.B. (1995) Effects of monovalent, exchangeable cations and electrolytes on the relation between swelling pressure and interlayer distance in montmorillonite. *Journal of Colloid and Interface Science*, **173**, 34–41.

(*Received 28 June 2015; revised 17 April 2017; Ms. 1018; AE: E. Ferrage*)